Sea Level and the Seasonal Fluctuations of the Equatorial Currents in the Western Pacific Ocean[1]

KLAUS WYRTKI

Dept. of Oceanography, University of Hawaii, Honolulu 96822

(Manuscript received 22 June 1973, in revised form 28 September 1973)

ABSTRACT

The seasonal variations of the dynamic topography relative to 500 decibars in the western equatorial Pacific, using data from 6900 hydrographic stations, are compared with the seasonal fluctuations of sea level observed at eleven islands. It is shown that the changes in the meridional profile of sea level correlate with changes in the strength of the major ocean currents measured by their speed or by geostrophic transports. The strength of the North Equatorial Current and that of the Countercurrent vary synchronously, both being strong in fall and weak in spring. The South Equatorial Current varies exactly out of phase with the two Northern Hemisphere currents, but is apparently in phase with the Undercurrent. Investigation of the particular example indicates that large anomalies seem to behave in the same fashion as the seasonal fluctuations of these currents.

1. Introduction

The purpose of this study is to demonstrate that observations of sea level at oceanic islands can be used to monitor the changes of the dynamic topography and to draw conclusions about changes in ocean circulation. Dynamic heights computed from observations made along the tracks of research ships give the dynamic topography and geostrophic transports only for that particular occasion, and many crossings of a current system are required to derive information about the seasonal and random changes of the current. The effort appears excessive. Sea level, on the other hand, can be conveniently and cheaply recorded on oceanic islands and along the continents to provide continuous information about its changes. It has been established by Wunsch (1972) for the example of Bermuda that fluctuations of sea level correlate highly with dynamic heights computed from the water structure, which means that there is a simple way to monitor the changes of geostrophic flow if suitably located islands are instrumented.

Most of the sea level gauges on oceanic islands are located in the western Pacific, in a region where strong zonal currents govern the circulation. Consequently, this region was selected to study the relationships between dynamic heights, sea level and circulation. Since hydrographic sections are very much scattered in time and space, and sea level data are readily available only in the form of monthly averages, it was not possible to compare the data from individual hydrographic sections with sea level observations on the same dates. Since annual variation is one of the most pronounced signals in all oceanic observations, I decided to explore the relations between these parameters using their seasonal cycle. Once a relationship has been established between dynamic height difference, sea level difference, and geostrophic flow for the seasonal cycle, it then becomes possible to use this relation to draw conclusions about the non-seasonal and long-term changes in ocean circulation, which is one of the goals of the North Pacific Experiment, NORPAX.

2. Data

Sea level observations for 10 oceanic islands in the western equatorial Pacific Ocean were available in the form of monthly mean values from the National Ocean Survey of NOAA. Most of these tide gauges have observations for the period 1951–71. The earlier years of these records have been analyzed by Roden (1963) and have been compared by means of cross spectra and spectral analysis with other parameters such as atmospheric pressure, sea temperature, and wind. Roden finds that in the equatorial zone the coherence between atmospheric pressure and sea level is poor, and consequently the sea level data have not been corrected for pressure.

Computed dynamic heights from 6900 hydrographic stations situated in the area between 30N to 20S and 140E to 140W, which overlaps the 10 sea level stations, were obtained from the National Oceanographic Data Center. They were sorted by months and averaged for areas of 2° latitude and 5° longitude. They form the basis on which a new map of dynamic topography is constructed for this area and from which profiles of dynamic height across the major current systems in the region have been derived.

[1] Hawaii Institute of Geophysics Contribution No. 572.

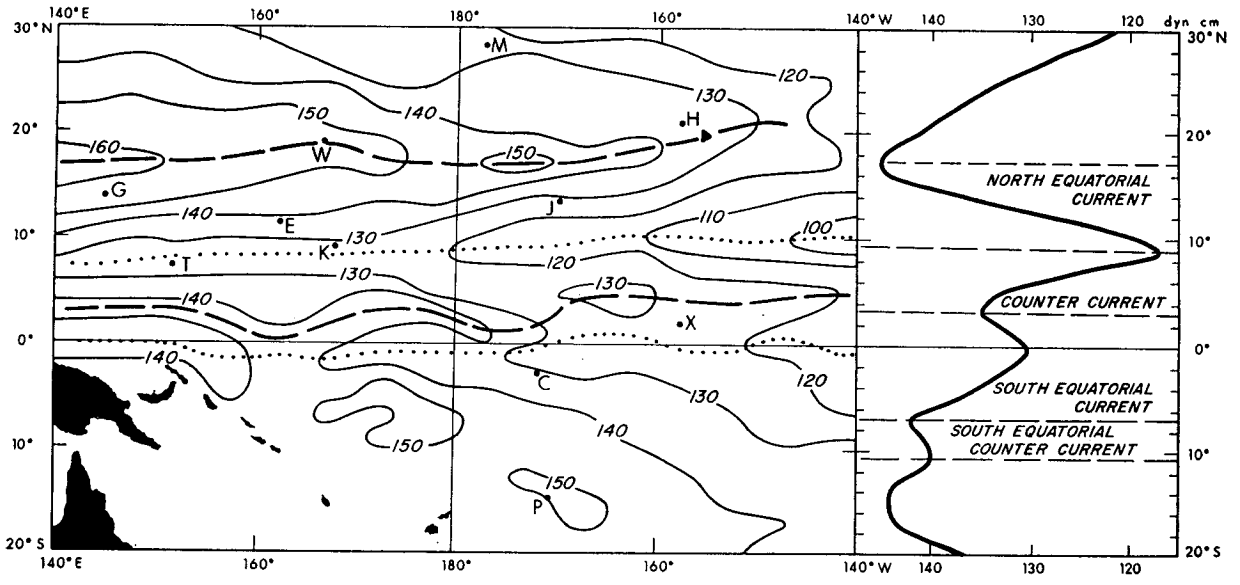

FIG. 1. Mean annual dynamic topography (cm) of the sea surface relative to 500 db in the western equatorial Pacific Ocean [left], and the zonally averaged mean annual profile [right]. The dashed and dotted lines represent the north equatorial ridge, the countercurrent trough, the equatorial ridge, and the equatorial trough. Letters give the location of sea level stations.

3. The dynamic topography in the western equatorial Pacific

The system of ridges and troughs in the topography of the sea surface connected with the equatorial circulation in the Pacific has been described by Reid (1961), but his analysis is based exclusively on the data from a number of carefully selected cruises. Since our study is aimed at unveiling the seasonal variations of the sea surface topography, it became necessary to use all the data available in the study area, which is that part of the western Pacific Ocean where long sea-level records from island stations are available. The area is bounded on the north by Midway, on the south by Samoa, on the east by the Hawaiian and Line Islands, and on the west by Guam (Fig. 1). The area covers all the main currents in the western equatorial Pacific, excluding only the strong western boundary currents, which affect meridional transports; also omitted from the study was the Coral Sea. The dynamic heights for all the hydrographic stations in an area bounded by 30N to 20S and 140E to 140W were computed relative to 1000 and 500 decibars (db) and averaged for each month and each rectangle of 2° of latitude and 5° of longitude. A selection of such a grid emphasizes the zonality of the distribution of dynamic height. A total of 5039 stations are available to chart the dynamic topography relative to 1000 db, but 6900 could be used to draw it relative to 500 db, increasing considerably the seasonal coverage in critical areas. Consequently, all of the following analyses use the topographies relative to 500 db, which have been found adequate for an investigation of geostrophic flow in the equatorial region by several investigators in the past (Montgomery and Stroup, 1962).

The annual mean dynamic topography relative to 500 db and a zonally averaged profile are shown in Fig. 1. This topography agrees rather well with the topography drawn by Reid (1961). The equatorial trough, the equatorial ridge near 3N, and the countercurrent trough between 8 and 10N are clearly shown and agree with Reid's map. No agreement is found in the vicinity of the north equatorial ridge, which is situated along 18–20N and stretches through the entire area from east of Hawaii to west of 140E. This ridge forms the northern boundary of the North Equatorial Current. North of it, but still under the trade-wind system, flows the Subtropical Countercurrent to the east (Yoshida and Kidokoro, 1967; Robinson, 1969). This north equatorial ridge is also clearly shown in the dynamic topography relative to 1000 db, although it is somewhat farther north at about 20N. In the map by Reid (1961) the ridge is not shown because of the paucity of data, and the center of highest dynamic topography shifts progressively north from 20N near Hawaii to 30N off Japan. The dynamic topographies shown in the various Kuroshio atlasses (Japanese Oceanographic Data Center, 1967, 1968, 1969) confirm the location of the ridge as represented in Fig. 1. The south equatorial ridge runs from the Solomon Islands to Tahiti, and the South Equatorial Countercurrent emphasized by Reid is not pronounced on the mean annual dynamic topography but appears in the zonally averaged topography. It might be variable in location and appears weakly developed on some of the monthly maps of dynamic topography, which were prepared, but are not shown here.

The average meridional profile of dynamic topography shows the various currents and the system of

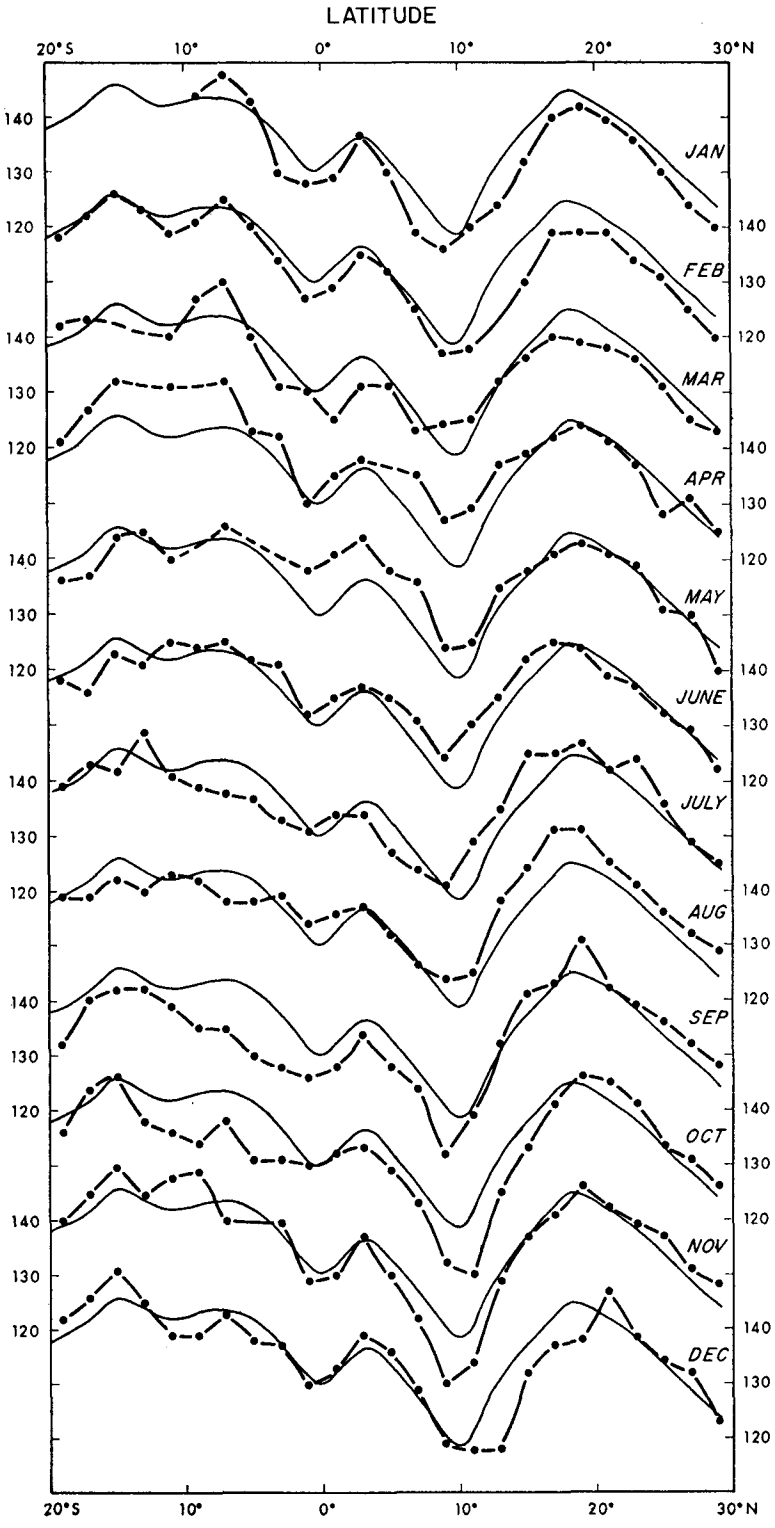

FIG. 2. Zonally averaged profiles of dynamic topography for each month compared with the mean annual profile (thin lines).

ridges and troughs very well (Fig. 1). It is virtually identical with the profile relative to 1000 db and differs by about 48 dynamic centimeters (dyn cm) in the belt between 20N and 20S. North of 20N the difference increases, and the slope of the topography relative to 500 db is stronger than that relative to 1000 db.

There is a general east–west slope of the sea surface throughout the area, but it is not consistent. The slope is generally stronger east of 170E and weaker west of 170E. Along the north equatorial ridge, sea level rises by about 40 cm between 140W and 140E, but the slope decreases north of the ridge, increasing to more than 50 cm near the center of the North Equatorial Current. Sea level in the Countercurrent trough rises by about 30 cm, but almost all of the slope is east of 170E, while the trough is essentially flat in the western part. It should also be noted that the Countercurrent trough shifts meridionally from 10N in the east to 8N in the west of the area. Most of the east–west slope along the equatorial ridge near 4N is found east of 180°, and like the Countercurrent trough it appears to be rather flat in the west. In the equatorial trough sea level slopes upward by about 25 cm from 140W to about 160E, where it apparently reaches a peak, and deepens again to the west. In the range of the South Equatorial Current sea level increases from east to west until it peaks in the south equatorial ridge running from the Solomon Islands to Tahiti.

4. The seasonal variations in dynamic topography

Zonally averaged profiles of dynamic topography are more suitable to show the seasonal fluctuations of the dynamic topography and of the associated circulation than are monthly charts of dynamic topography, which, especially south of the equator, suffer from gaps in data coverage. When compared with the mean annual profile (Fig. 2), the changes in these monthly profiles during the year are quite pronounced. The north equatorial ridge is stronger in summer (June through September) and weaker in winter (December through March), which might largely be attributed to the heating and cooling cycle and the corresponding changes of steric sea level. The Countercurrent trough is deeper than normal from September through February and shallower from March to July. Since these changes are not in phase, they cause fluctuations in the strength of the North Equatorial Current, making it comparatively weak from March to July and stronger from September through November.

Fluctuations of the dynamic topography near and south of the equator are not so reliably represented, because gaps in the data give unequal weight to observations either in the eastern or in the western parts of the area. I do not believe that a more sophisticated analysis based on interpolation between stations rather than on a straight averaging would have improved the profiles, but rather that it might introduce artificial features. Consequently, we will discuss the data as given, keeping in mind the limitations due to paucity. The equatorial ridge and the equatorial trough appear in all monthly profiles, although their intensity varies considerably. Higher sea level in the equatorial ridge in November and December leads to an intensification of the Countercurrent, while lower sea level in February and March causes it to weaken. The equatorial trough is more pronounced from November through March, and more weakly developed during the remainder of the year. The slope connected with the South Equatorial Current is rather well developed from January to April, and is rather weak from May to August.

In spite of the large total number of hydrographic stations used, their distribution in time and space is not sufficient to draw clearly defined profiles of dynamic topographies for the area south of the equator; and even near the equator, where gradients are small, fluctuations in the size of the data sample may cause some bias. Moreover, it should be borne in mind that the observations at a hydrographic station really represent only the situation at a given instant, and that many stations would be required to derive a monthly mean with a statistical accuracy of about ± 2 dyn cm. In contrast, observations of sea level represent a continuous record at a fixed location, and the computed monthly means of sea level over several years give a very reliable record of the mean seasonal fluctuation.

The mean seasonal variation of the profile of dynamic topography averaged zonally between 170E and 140W over 50° of longitude is shown in Fig. 3 to demonstrate the behavior of the various ridges and troughs in time. Compared with this isopleth diagram is a corresponding diagram showing the deviation of the monthly mean sea level from the long-term mean at seven island stations forming a north–south section in the same area. Sea level at Midway, Honolulu, and Johnston varies almost synchronously; it is lowest in spring and highest in late summer. The dynamic topography of the ridge has a similar seasonal variation, which reflects the heating and cooling cycle. Sea level in the Countercurrent trough, represented by Kwajalein, is highest in spring and lowest in winter. This trend is indicated in the isopleths of dynamic topography, but relatively large noise in the data and a contour interval of 10 dyn cm does not lend itself to an easy comparison. Neither of the stations Christmas and Canton on opposing sides of the equator is situated exactly in the equatorial ridge or in the trough, but both exhibit a very high correlation, indicating that sea level over the entire equatorial region varies synchronously. The agreement with the averaged dynamic topography is limited, chiefly due to the excessive noise in the zonally averaged dynamic height values. Near the south equatorial ridge sea level at Pago Pago indicates high values from April to September and lowest values in December and January, while the corresponding high and low values in the dynamic topography appear to occur earlier.

When assessing these diagrams it should be noted that sea level anomalies are contoured at 2-cm intervals, while those of dynamic height are contoured at 10-cm intervals because of the strong gradients and the high noise in the data. Since the mean seasonal variations of

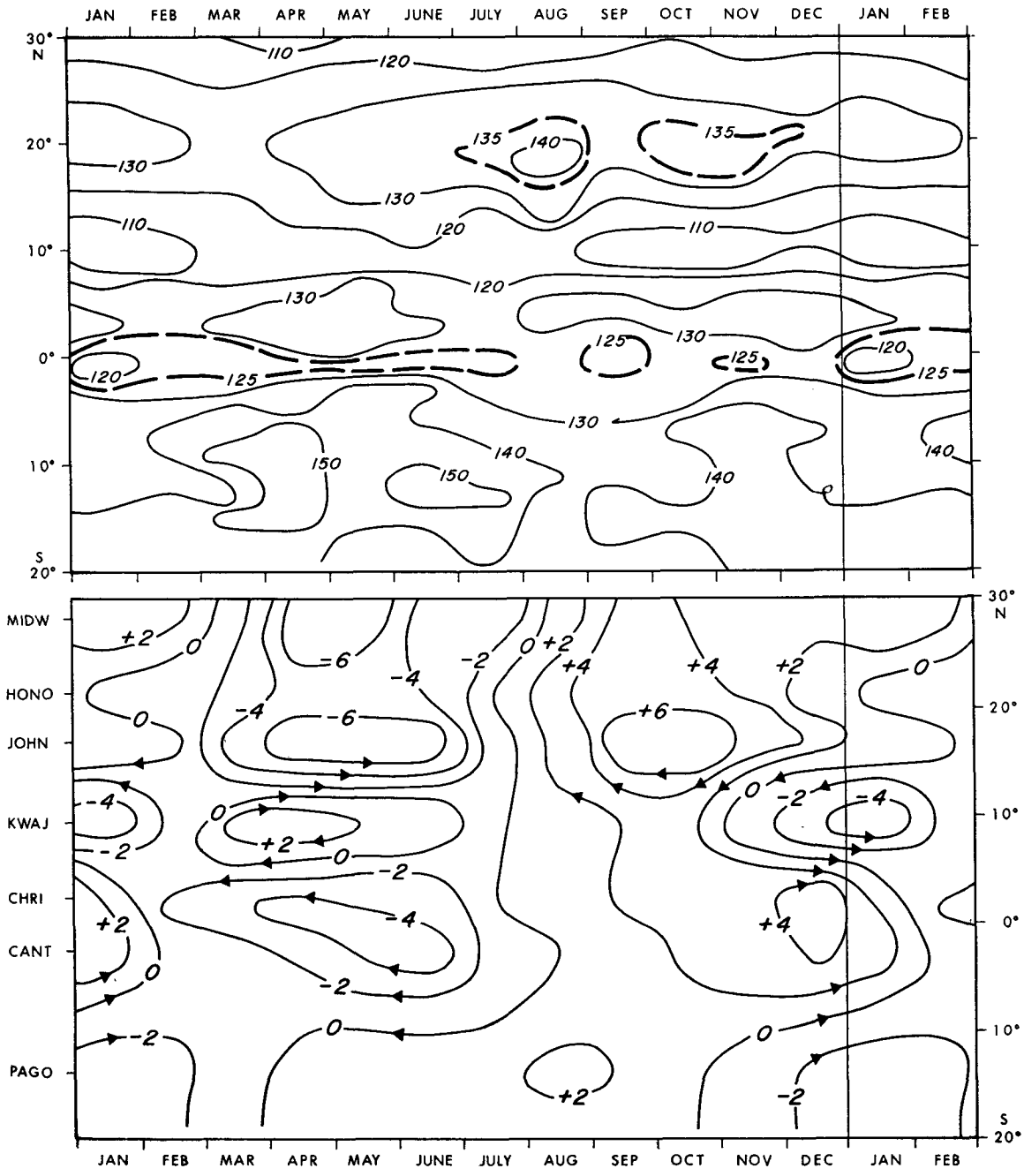

FIG. 3. Isopleths of zonally averaged dynamic topography (cm) relative to 500 db (upper) and of the mean monthly deviation of sea level from the annual mean (cm) at seven island stations (lower). Arrows on the lower diagram indicate abnormal zonal flow.

sea level are more reliably derived from observations than are the average dynamic heights, as pointed out above, I prefer to give them a greater weight.

It might be appropriate to estimate at this point the accuracy of observations of sea level and of dynamic topography. Sea level is observed continuously, with daily mean sea level being computed from 24 hourly readings and the monthly mean from 30 daily means. Assuming an accuracy of ± 10 cm for the individual hourly reading, the precision of the monthly mean is ± 0.36 cm. Tide gauges usually record at a 1:5 reduction and if the reading on the chart paper is accurate to ± 0.2 cm and the zero point of the paper on the recording drum is accurate to the same amount, the actual error in mean sea level is about ± 1 cm. A further indirect evidence with regard to the accuracy of mean sea

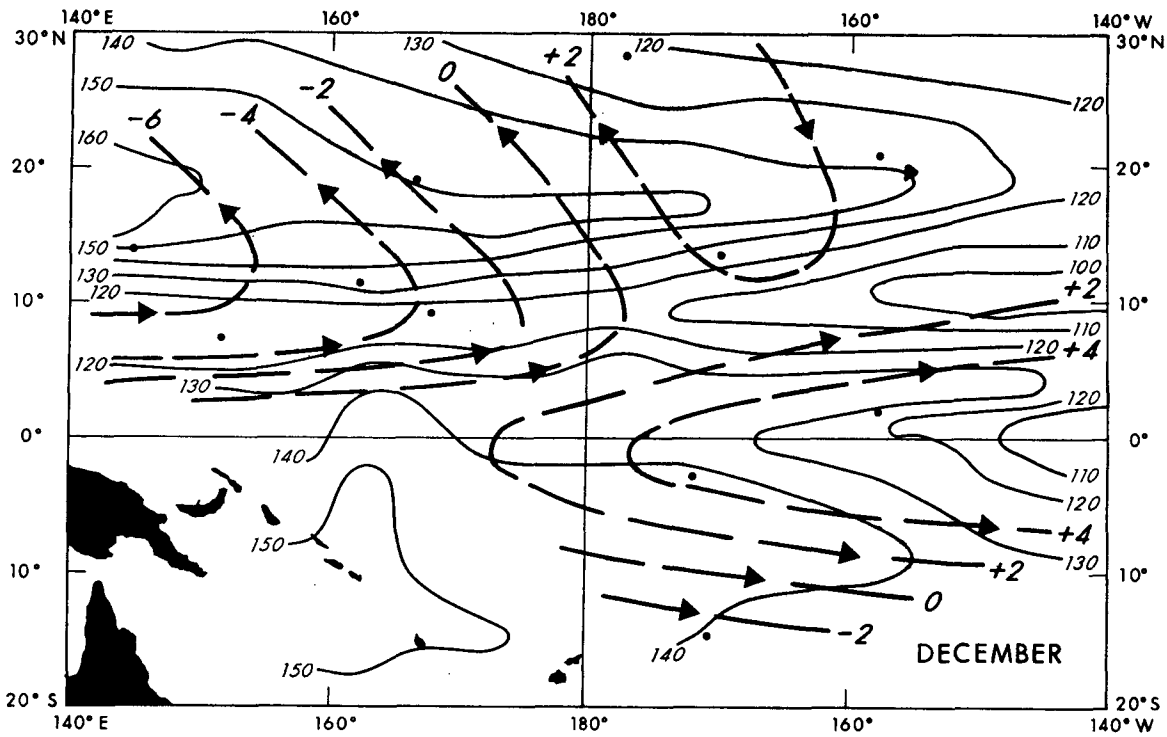

FIG. 4. Dynamic topography of the sea surface relative to 500 db for December (thin lines) and deviations of mean December sea level from the annual mean (heavy broken lines). Arrows indicate anomalous flow.

level observations lies in the fact that long-term changes of sea level at stations as far apart as Christmas and Canton Island agree to within ±2 cm. Therefore, it can be concluded that the monthly mean of sea level at a given island is know to better than ±2 cm. The same is not true for the values of dynamic topography, which constitute single observations at an arbitrary instant of time. Dynamic topography at a given location can change by ±10 cm within hours due to internal waves, and by a similar amount over distances of 50 km due to the presence of geostrophic eddies. The error of the mean of 10 observations is ±3.3 cm, and one might conclude that the mean dynamic topography based on 10 observations per grid point is only accurate to about ±5 cm, a conclusion which is well supported by the curves shown in Fig. 8. Consequently, the sea level data represent a much more precise set of data than the dynamic topographies.

The variations of sea level at stations representing the different ridges and troughs in the dynamic topography are not in phase; consequently, the slopes in sea level across the various current systems change with the season. It is quite apparent that the low sea level at the north equatorial ridge and the high sea level in the Countercurrent trough from March to June decrease the slope across the North Equatorial Current and its flow. High sea level at the north equatorial ridge from August to November, and low sea level at the Countercurrent trough from November to January increase the flow in the North Equatorial Current during this time as indicated by arrows in Fig. 3. In the same fashion, Countercurrent flow is decreased from March to June by high sea level in the Countercurrent trough and low sea level near the equator. Countercurrent flow is increased from November to January, when sea level is high near the equator and low in the Countercurrent trough. The South Equatorial Current is strengthened by a larger sea level difference between the south equatorial ridge and the equatorial trough from April to June, and weakened from November to February.

The foregoing analysis of the seasonal changes of the equatorial circulation shows that the North Equatorial Current and the Countercurrent fluctuate synchronously, chiefly in response to the sea level fluctuations in the Countercurrent trough. The South Equatorial Current seems to fluctuate out of phase with the North Equatorial Current. This important result can be illustrated even more dramatically, when seasonal departures of sea level from its mean are contoured in horizontal maps, and are compared with the dynamic topography of the corresponding month (Figs. 4 and 5). As examples, the months of December and April have been selected, where sea level departures are at a maximum.

In December sea level is low near the Countercurrent trough and near the south equatorial ridge, and it is high near the equator and in the eastern part of the north equatorial ridge. The contours of sea level departure or of anomalies of sea level topography can be interpreted as anomalous flow in the same way as

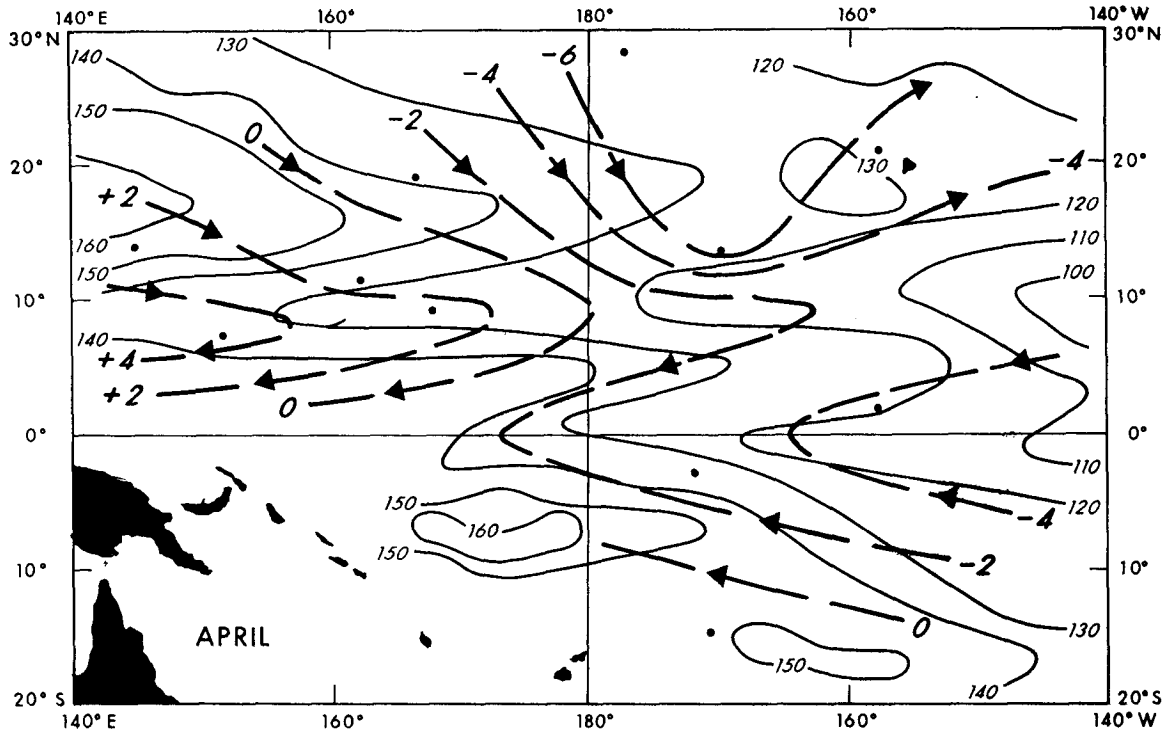

FIG. 5. As in Fig. 4 except for April.

atmospheric pressure anomaly patterns. In the map for December (Fig. 4) the strengthening of the Countercurrent is clearly shown, as well as the weakening of the South Equatorial Current (indicated by arrows). At the same time the east-west slope in the north equatorial ridge is weakened and the North Equatorial Current is somewhat intensified and is strongly zonal. This zonality of the flow of all currents in December is especially apparent when comparing the dynamic topography for December with that for April.

In April (Fig. 5) sea level is low in the eastern portion of the north equatorial ridge and near the equator, and high in the Countercurrent trough and near the south equatorial ridge. This situation implies an intensification of the east–west slope and a general flow toward the equator. It leads to a simultaneous weakening of the North Equatorial Current and of the Countercurrent, and to a strengthening of the South Equatorial Current. The change in the dynamic topography is also quite striking, and indicates a decreased zonality of the circulation with strong equatorward flow across the north equatorial ridge. The discussion of these two cases demonstrates quite clearly that relatively small changes in sea level can have a pronounced effect on the circulation pattern and its strength, and that not only the meridional, but also the zonal slopes are changed.

5. North Equatorial Current and Countercurrent

Seasonal variations in the flow of the Countercurrent have been known for a long time (Puls, 1895) and have recently been connected with fluctuations in the slope of sea level across the current (Wyrtki, 1973). Fluctuations in the strength of the North Equatorial Current have been suspected, but have not been documented until lately (Seckel, 1968, 1972). He finds from data taken during the Trade Wind Zone Investigation near Hawaii, that flow in the North Equatorial Current is weaker in spring and stronger in fall. Relations between the dynamic topography associated with the North Equatorial Current and the Countercurrent and sea level differences across these two currents are explored in Figs. 6 and 7, respectively, representing the situation in the western part (140E–180E) and the central part (180W–140W) of the Pacific. The dynamic topographies were averaged zonally for each month and for the longitudes specified above, and their seasonal variations at the north equatorial ridge, at the Countercurrent trough, and at the equatorial ridge are shown. The strongest seasonal signal is always found at the Countercurrent trough. The difference of dynamic height across the North Equatorial Current between the ridge and the trough varies from a minimum of 22 cm in spring to a maximum of 37 cm in fall in the western Pacific and slightly more in the central Pacific. This variation is substantial and reflects a strong seasonal change in the flow of the North Equatorial Current. From a comparison of the curves for the two regions it is obvious that the period of weak flow is short in the western Pacific (March to May), while in the central Pacific the period of strong flow is short but lasts longer until January.

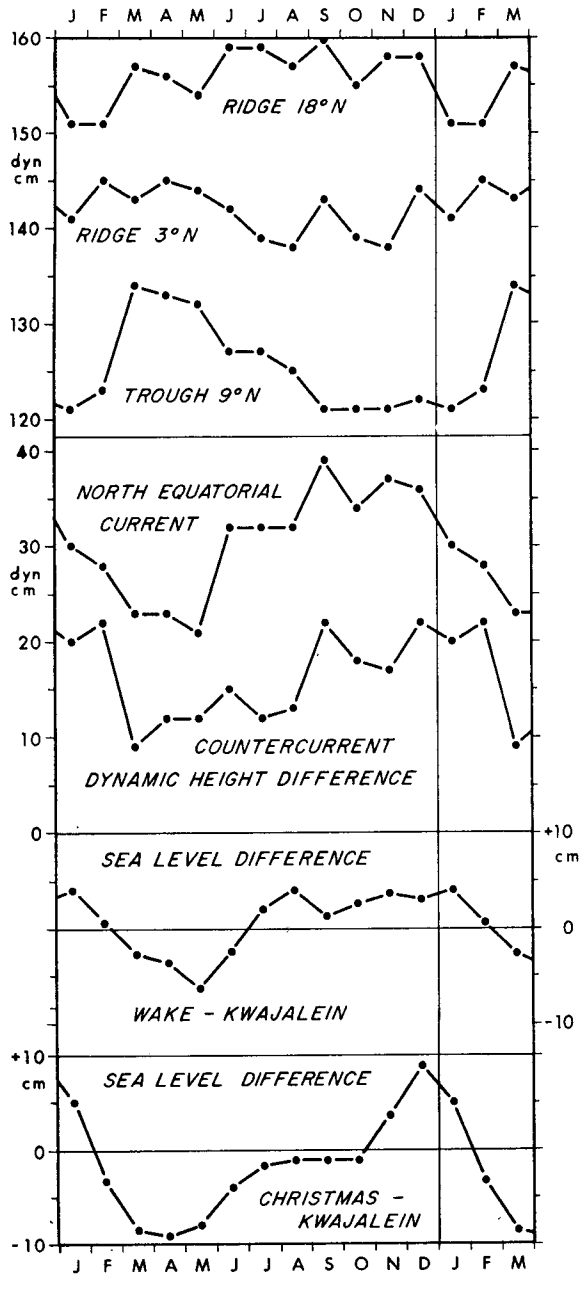

FIG. 6. Mean seasonal variations of dynamic topography, dynamic height difference, and sea level difference in the western Pacific. Upper part: dynamic height in the north equatorial ridge (18N), in the Countercurrent trough (9N), and in the equatorial ridge (3N). Central part: dynamic height difference across the North Equatorial Current and the Countercurrent. Lower part: sea level differences between Wake and Kwajalein and between Christmas and Kwajalein.

The differences of dynamic height across the current are compared with the sea level differences between Wake (19N) and Kwajalein (9N), and both show the same seasonal cycle. The range of the sea level difference (10 cm) is somewhat smaller than that of the dynamic height difference (14 cm), which may indicate that the sea level difference between the two gauges does not always include the entire North Equatorial Current. For the central Pacific, the difference of dynamic height is compared with the difference of sea level between Honolulu (21N) and Kwajalein (9N). In this case both curves have the same range, indicating that the North Equatorial Current always flows south of the Hawaiian Islands. The seasonal variations of the two curves exhibit remarkable agreement and demonstrate that changes in the slope of dynamic topography across the North Equatorial Current can be continuously monitored by the sea level difference between Wake and Kwajalein or between Honolulu and Kwajalein. Unfortunately, no island is situated near 10N south of Hawaii to monitor sea level in the Countercurrent trough at this meridian.

The seasonal variation of the Countercurrent according to the difference of dynamic height between the Countercurrent trough and the equatorial ridge is also shown in Figs. 6 and 7. In the western Pacific this difference varies between 10 and 22 cm, while in the central Pacific it is higher, varying between 15 and 30 cm. The period of weak Countercurrent flow apparently lasts longer in the western than in the central Pacific. The sea level difference between Christmas Island (2N) and Kwajalein (9N) (which is presently the only suitable station pair to monitor the Countercurrent) has a similar seasonal variation but the variations of the dynamic height difference do not agree as well as the corresponding curves for the North Equatorial Current. The reason for this lack of good agreement is probably due to an inadequate number of dynamic height observations in the vicinity of the equatorial ridge. Again, I would like to claim that the seasonal fluctuation of sea level and its differences are established with a greater precision than are those of dynamic topography. Moreover, it has been demonstrated (Wyrtki, 1973) that the sea level difference across the Countercurrent correlates extremely well with the geostrophic transports and surface current speed.

These comparisons between dynamic height differences and sea level differences for the North Equatorial Current and the Countercurrent confirm the earlier observation that the strengths of the two currents fluctuate almost synchronously. Both currents are weak in spring, the Countercurrent increasing somewhat later than the North Equatorial Current; both currents reach maximum strength in fall, with the Countercurrent appearing to remain strong somewhat longer. This synchronous seasonal fluctuation indicates a strong coupling between the two currents, apparently governed by the intensity of the Countercurrent trough, but the mechanism and the reasons for the synchroneity are not yet clear.

The sea level difference and the difference of dynamic heights across the North Equatorial Current can now be compared with geostrophic transport calculations.

During the Trade Wind Zone Investigation (Seckel, 1968) 16 surveys crossing the North Equatorial Current were made between February 1964 and June 1965. The computed geostrophic transports relative to 1000 db between the north equatorial ridge and the Countercurrent trough are also shown in Fig. 7. The seasonal variations of the transports reflect very well those of dynamic height difference as well as those of the sea level difference between Honolulu and Kwajalein. This correspondence implies that the slope of the sea surface represents not only the geostrophic surface current, but also the transport of a chiefly baroclinic ocean current. The density structure in the North Equatorial Current consists of a relatively thin warm surface layer of low density above the denser deep layer. The transport is proportional to the slope of the interface between the two layers muiltplied by the thickness of the upper layer. The mean thickness of the upper layer changes very little, because it is climatically controlled by the amount of warm water in the entire subtropical gyre. Consequently, slope and transport are essentially directly related.

The strength of an ocean current can either be measured by its surface speed or by its transport. The equatorial currents are currents of the upper layer of the ocean (Montgomery and Stroup, 1962) and most of their transport is in the upper few hundred meters. Although flow in these equatorial currents may occasionally have the same direction from the sea surface to the bottom in great depth, I do not consider the water movements below about 500 m depth to be part of the equatorial currents. Flow below this depth belongs to the intermediate or deep water circulation and should not be included into an estimate of the circulation in the surface layer. By establishing the close correspondence between variations in sea level and in dynamic height, the earlier conclusion by Wunsch (1972) is confirmed, that sea level changes are essentially steric. The fact that independent observations of sea level difference, surface current speed, and geostrophic transports correlate as well as one can possibly expect from geophysical variables of this nature, means that each of them can be regarded as a measure of the strength of a current. The present study indicates that sea level differences are most suitable to monitor the changes of the strength of these currents.

6. The South Equatorial Current

The area under study covers only the western portions of the South Equatorial Current, where it is much weaker than in the eastern half of the ocean, where during part of the year the South Equatorial Countercurrent is found, and where unfortunately the data coverage is rather poor. Moreover, parts of the South Equatorial Current flow on both sides of the equator and surface current speeds are generally highest close to the equator, where strong zonal currents are associated with only very minute meridional slopes. Consequently, it is not possible to relate the flow near the

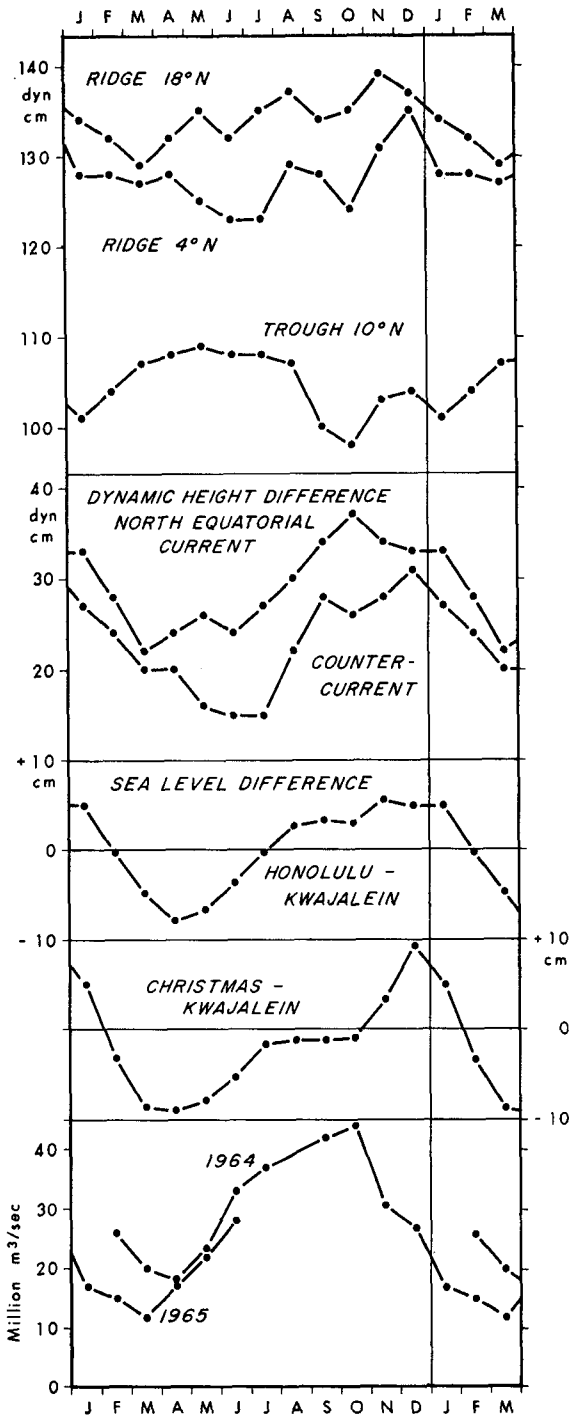

FIG. 7. Mean seasonal variations of dynamic topography, dynamic height difference, and sea level difference in the central Pacific. Upper part: dynamic height in the north equatorial ridge (18N), in the Countercurrent trough (10N), and in the equatorial ridge (4N). Central part: dynamic height differences and sea level differences across the North Equatorial Current and the Countercurrent. Lower part: geostrophic transports of the North Equatorial Current in 1964 and 1965.

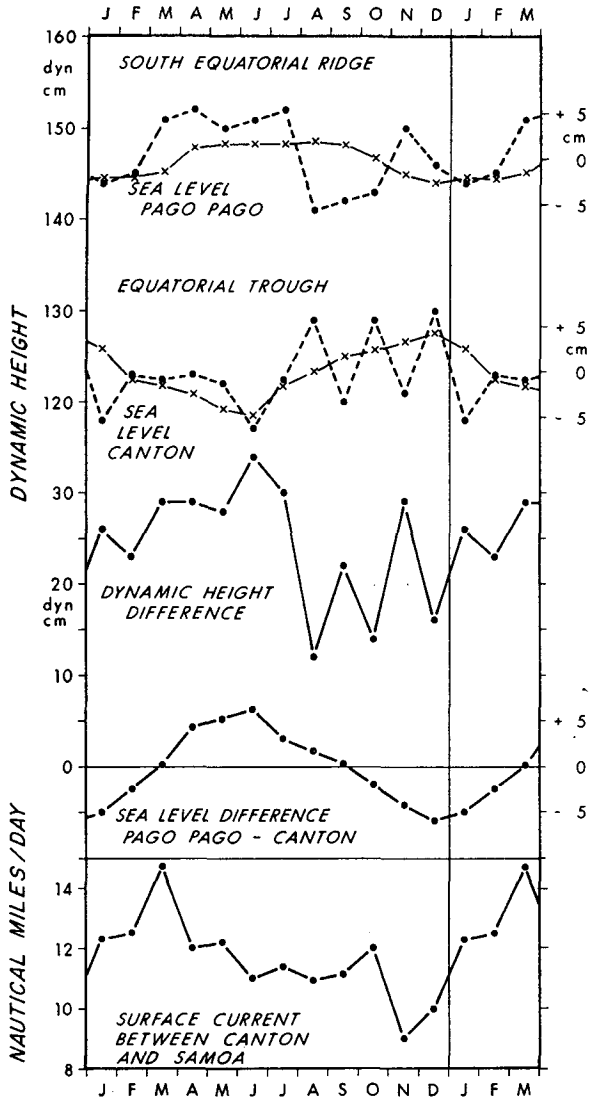

FIG. 8. Mean seasonal variations of dynamic height, sea level and surface currents in the South Equatorial Current. Upper part: dynamic topography in the south equatorial ridge compared with sea level at Pago Pago and dynamic topography in the equatorial trough compared with sea level at Canton. Central part: dynamic height difference compared with sea level difference. Lower part: surface current between Canton and Samoa.

equator to observed sea level differences in order to draw conclusions about the seasonal variations of the current.

The other portion of the South Equatorial Current, which is situated entirely south of the equator can, however, be conveniently monitored by the sea level difference between Canton (3S) and Pago Pago (14S). Changes in sea level difference here should adequately represent the changes in the slope across that portion of the South Equatorial Current which is situated between the equatorial trough and the south equatorial ridge (Fig. 1). It is evident that some disturbance will be caused by the appearance of the South Equatorial Countercurrent between 8 and 10S, which was found by Merle *et al.* (1969) to be rather variable, but almost always present at 170E. Farther to the east, near 170W, the South Equatorial Countercurrent seems to be more pronounced during the first half of the year and mostly absent during the second half, but data are rather scanty.

The seasonal variations of the dynamic height zonally averaged between 170E and 140W over 50° of longitude are shown in Fig. 8 for the south equatorial ridge and for the equatorial trough. They are compared with those of sea level at Canton and Pago Pago, and it is quite apparent that the dynamic heights are very noisy due to the small data sample on which they are based. The general seasonal trend is, however, reasonably well reflected. It is apparent that the seasonal oscillations of sea level at the two stations are almost opposite, and consequently the sea level difference between them fluctuates appreciably. The dynamic height difference, representative of the geostrophic flow in the South Equatorial Current (also shown in the figure), is about 30 cm from March to July and 20 cm from August to December. The seasonal variation of the sea level difference shows a maximum in June and a minimum in December. Surface current speed between Canton and Samoa, evaluated from the *Atlas of Surface Currents for the Southwestern Pacific Ocean* (U. S. Navy Hydrographic Office, 1944), is also shown in Fig. 8 and indicates strongest flow in March and weakest flow in November. In spite of the large scattering of the dynamic height difference, the three curves exhibit a common trend, and indicate that the flow in the South Equatorial Current between Canton and Samoa is strong from March to July and weak from October to February. This seasonal variation in the strength of the South Equatorial Current is opposite to that of the Countercurrent and the North Equatorial Current, an important result, which might point to interactions among the equatorial currents, and is worthy of further study.

7. Seasonal changes of the equatorial currents

After the relation between sea level difference and flow in the three main equatorial surface currents has been established, it is now possible to use the mean observed profile of dynamic topography and superimpose on it the monthly deviations of observed sea level to derive the actual monthly profile of the sea surface. In Fig. 9 the mean monthly departures of sea level from their annual mean have been superimposed on the annual mean profile of dynamic height, averaged between 140 and 180E. It is implied that these curves represent the actual profile of sea level, and may now be used to interpret the strength of the various currents.

It is quite apparent from these sea level profiles that the North Equatorial Current is strongest from August

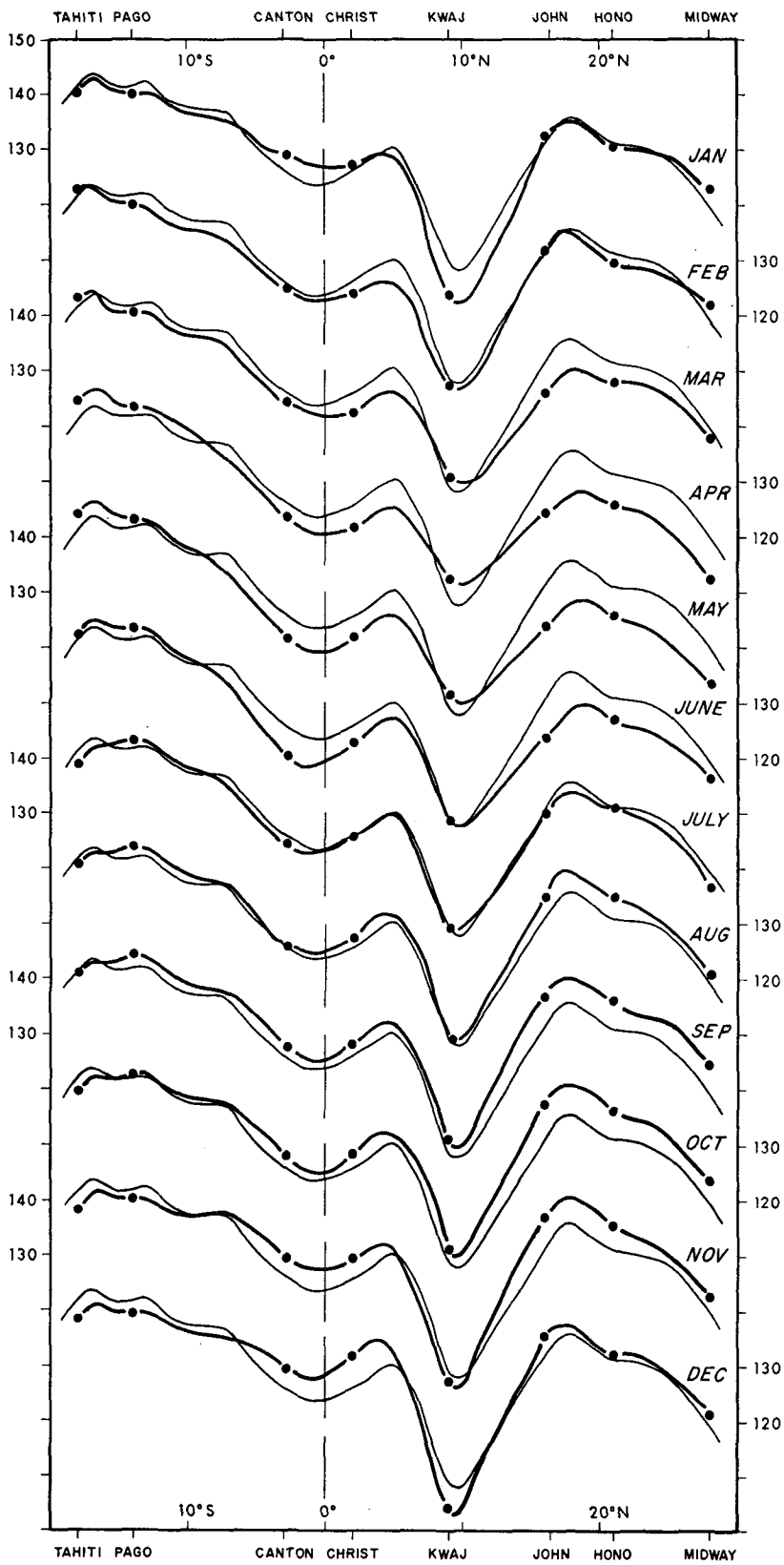

FIG. 9. Monthly profiles of sea surface topography composed from the mean annual profile of dynamic height averaged between 140W and 180W (thin lines), and the mean monthly deviation of sea level from the annual mean at eight sea level stations.

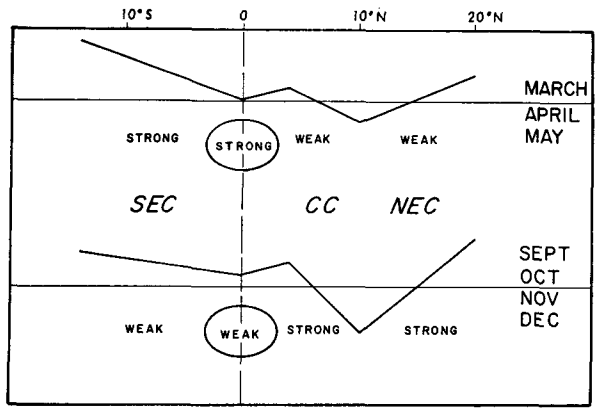

FIG. 10. Schematic diagram of the profile of sea level and the strength of the equatorial currents in spring and fall.

to January, and that from March to June it is much weaker than normal. The Countercurrent is strongest from November to January and rather weak from February to June. The fluctuations of these two currents are essentially synchronous. Near the equator, sea level is lower than normal during the first half of the year, and higher during the second half. The slope across the South Equatorial Current is intensified from April to July and weakened from October to January. This implies that, at least in the western Pacific, fluctuations of the South Equatorial Current are exactly opposite those of the North Equatorial Current and Countercurrent. In this connection it is interesting to note that at least as far as the few direct measurements would indicate, the Equatorial Undercurrent appears to be stronger in northern spring and weaker in fall (Taft and Jones, 1973). This would imply that Undercurrent fluctuations are synchronous with those of the South Equatorial Current. Indirect evidence for such fluctuations in the strength of the Undercurrent is also available from the sea level data. In Figs. 4 and 5 the contours of anomalous sea surface topography show divergent movements away from the equator in December, when the Undercurrent should be weak, and convergent movements toward the equator in April, when it is supposedly strong. It will be interesting to see whether future observations and analysis of the Undercurrent will confirm this observation. The volume transports of the Undercurrent at 170E quoted by Hisard *et al.* (1970) cover only the period March through August, and no seasonal signal is apparent because of large transport fluctuations.

The results concerning the seasonal fluctuations of the strength of the four equatorial currents can now be combined to discuss the fluctuations of the entire equatorial current system, and some surprising relations become apparent. The two Northern Hemisphere currents, the North Equatorial Current and the Countercurrent fluctuate in phase, and so does the Southern Hemisphere system composed of the South Equatorial Current and the Undercurrent. The system of the Southern Hemisphere is, however, out of phase with the system of the Northern Hemisphere. Fig. 10 illustrates the strength of the currents and the schematic sea level profiles for spring and fall. Each system consists of westward and an eastward flow, which fluctuate synchronously; the two systems fluctuate almost exactly out of phase.

This remarkable conclusion about the coupling of the equatorial currents, although not yet fully substantiated, may have important consequences for the understanding and the explanation of anomalous events in the equatorial current system. If anomalies are coupled in the same fashion as the annual cycle, one should expect to observe during an El Nino a strong Countercurrent, a weak South Equatorial Current, and a weak Undercurrent. Such a situation is exactly described by Austin (1960) for December 1957 when equatorial upwelling ceased; the Undercurrent was apparently weak, as was the South Equatorial Current, and the Countercurrent was very strong and extended almost to the equator. Coinciding with this development of the equatorial currents was a strong El Nino off Peru. Bjerknes (1966) has discussed the large-scale ocean-atmosphere interactions accompanying the 1957–58 event. This single example demonstrates that an analysis and understanding of the seasonal fluctuations of the equatorial currents can be used to study their relations during abnormal periods, too, but research on such anomalous situations is still in progress. It is not yet clear at this time, how the fluctuations in the strength of the North and South Equatorial Currents are related to those of the wind systems, and research on these relations will be reported later.

In summary, the following conclusions can be drawn:

1) Departures of observed sea level at island stations can be used to monitor the changes of the dynamic topography and consequently those of major current systems.

2) The North Equatorial Current and the Countercurrent fluctuate synchronously, both being strong in fall (September to December) and weak in spring (March to May).

3) Fluctuations of their transport can be monitored by sea level differences.

4) The South Equatorial Current and the Undercurrent are also in phase, but fluctuate out of phase with the two currents in the Northern Hemisphere.

5) Large anomalies in the major currents apparently behave in the same fashion as their seasonal fluctuations.

Acknowledgments. This research was supported by the National Science Foundation and the Office of Naval Research under the North Pacific Experiment of the International Decade of Ocean Exploration. This support is gratefully acknowledged.

REFERENCES

Austin, T. S., 1960: Summary, 1955–57 ocean temperatures, Central Equatorial Pacific. *Calif. Cooperative Oceanic Fisheries Invest. Rep.*, **7**, 52–55.

Bjerknes, J., 1966: A possible response of the atmospheric Hadley circulation to equatorial anomalies of ocean temperature. *Tellus*, **18**, 820–829.

Hisard, P., J. Merle and B. Voituriez, 1970: The Equatorial Undercurrent at 170°E in March and April 1967. *J. Marine Res.*, **28**, 281–303.

Japanese Oceanographic Data Center, 1967, 1968, 1969: Cooperative study of the Kuroshio Atlas.

Merle, J., H. Rotschi and B. Voituriez, 1969: Zonal circulation in the tropical western South Pacific at 170°E. *Bull. Japanese Soc. Fisheries Oceanogr.*, Special number, Prof. Uda's Commemorative Papers, 91–98.

Montgomery, R. B., and E. D. Stroup, 1962: Equatorial waters and currents at 150°W in July–August 1952. *The Johns Hopkins Oceanogr. Studies*, No. 1, 68 pp.

Puls, Caesar, 1895: Oberflachentemperaturen und Stromungsverhaltnisse des Aquatorialgurtels des Stillen Ozeans. *Archiv. Deut. Seewarte*, **18**, No. 1, 38 pp.

Reid, J. L., 1961: On the geostrophic flow at the surface of the Pacific Ocean with respect to the 1,000-decibar surface. *Tellus*, **13**, 489–502.

Robinson, M. K., 1969: Theoretical predictions of subtropical countercurrent confirmed by bathythermograph (BT) data. *Bull Jap. Soc. Fisheries Oceanogr.*, Special number, Prof. Uda's Commemorative Papers, 115–121.

Roden, Gunnar I., 1963: On sea level, temperature, and salinity variations in the central tropical Pacific and on Pacific Ocean Islands. *J. Geophys. Res.*, **68**, 455–472.

Seckel, G., 1968: A time-sequence oceanographic investigation in the North Pacific trade-wind zone. *Trans. Amer. Geophys. Union*, **49**, 377–387.

——, 1972: Hawaiian-caught skipjack tuna and their physical environment. *Fishery Bull.*, **72**, 763–787.

Taft, B. A., and J. H. Jones, 1973: Measurements of the equatorial undercurrent in the Eastern Pacific. *Progress in Oceanography*, Vol. 6, New York, Pergamon Press.

U. S. Navy Hydrographic Office, 1944: *Atlas of Surface Currents, Southwestern Pacific Ocean*. H. O. Publ. 568.

Wunsch, C., 1972: Bermuda sea level in relation to tides, weather, and baroclinic fluctuations. *Rev. Geophys. Space Phys.* **10**, No. 1, 49 pp.

Wyrtki, K., 1973: Teleconnections in the equatorial Pacific Ocean. *Science*, **180**, 66–68.

Yoshida, K., and T. Kidokoro, 1967: A subtropical countercurrent (II)—A prediction of eastward flows at lower subtropical latitudes. *J. Oceanogr. Soc. Japan*, **23**, 231–246.